

**Supplemental Figure S1.  $TNF^{\Delta ARE/+}$  mice display gender differences in disease severity and phenotype of GALT Tregs.** (A) Histologic evaluation of ileal inflammation in young (<10 wks) and old (>10 wks) cohorts of  $TNF^{\Delta ARE/+}$ -M and -F mice (n=24/group) shows increased disease severity in females (left). Representative photomicrographs of H&E-stained ilea from 16-wk-old  $TNF^{\Delta ARE/+}$ -M and -F mice are shown (right; scale bar = 100  $\mu$ m; X20 + 1.25 original magnification). (B) 16-wk-old  $TNF^{\Delta ARE/+}$ -M mice express an increased percentage of Treg cells ( $CD25^+Foxp3^+$ ) within the MLN  $CD4^+$  T cell population by flow cytometry (left, n=6/group). Representative histograms show CD25 and Foxp3 expression within the  $CD4^+$  population (right).

**Supplemental Figure S2. FACS sorting scheme for isolation of  $CD45RB^{hi}$  and  $CD45RB^{low}$  cells.**  $CD4^+CD45RB^{hi}$  and  $CD4^+CD45RB^{low}$  cells were isolated from SAMP-M and -F mice by fluorescence activated cell sorting. Figure shows sequential gating on lymphocytes by FSC-A and SSC-A, followed by exclusion of aggregates by

SSC-W and SSC-A. Singlet lymphocytes were selected on CD4 positive fluorescence and then CD45RB high and low expression.

**Supplemental Figure S3: Treg cells from SAMP-M show enhanced ability to suppress proinflammatory cytokines and MPO in *in vivo* adoptive transfer model.**

Colon tissues and MLNs were harvested from mice 8 weeks after adoptive transfer, and MLN cells were activated *in vitro* with  $\alpha$ CD3/ $\alpha$ CD28. MPO activity in colon tissues and cytokine secretion from activated MLN cells are expressed as mean  $\pm$  SEM (\* $p$ <0.05 and \*\* $p$ <0.01 compared to CD45RB<sup>hi</sup> group; n=16/group).

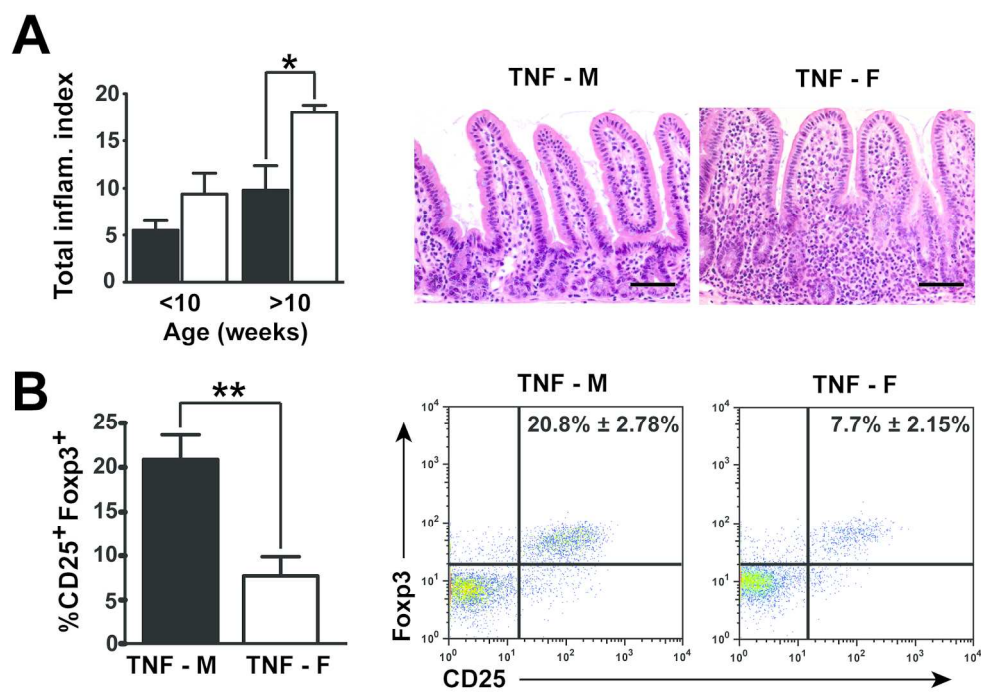
**Supplemental Figure S4. FACS sorting scheme for isolation of Tconv and Treg cells.**

CD4<sup>+</sup>CD25<sup>-</sup> Tconv and CD4<sup>+</sup>CD25<sup>+</sup> Treg cells were isolated from SAMP-M and – F mice by fluorescence activated cell sorting. Figure shows sequential gating on lymphocytes by forward (FSC-A) and side (SSC-A) scatter, followed by exclusion of aggregates by SSC-W (width) and SSC-A (area). Singlet lymphocytes were selected on CD4 positivity and then CD25 high expression (approximately top 10% of CD25-positive population).

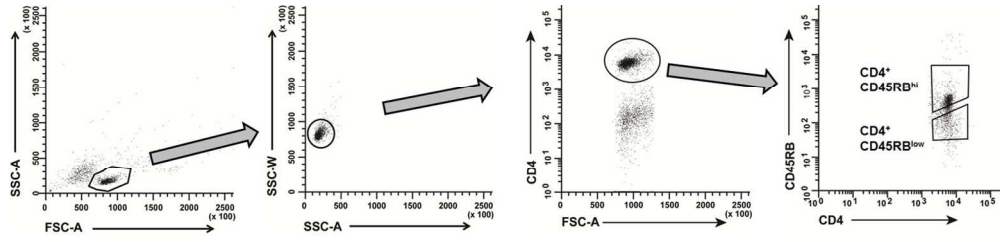
**Supplemental Figure S5. Serum estrogen levels are comparable in SAMP versus AKR mice, post-puberty.** Serum estrogen levels were measured in SAMP and AKR

male and female mice at 6 and 14 weeks of age. Levels are presented as mean  $\pm$  SEM; significance is based on two-tailed Student's t-test with Welch's correction (\* $p < 0.05$ ,  $n = 8-10$ /group).

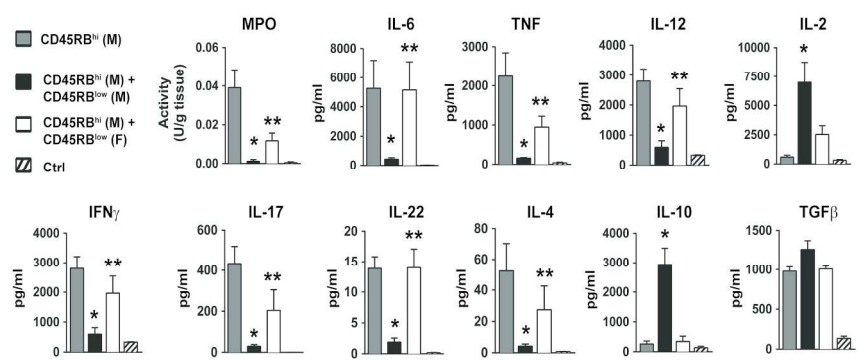
**Supplemental Figure S6. Gender does not influence *in vivo* permeability.** (A) *In vivo* permeability of 4-5 week old AKR and SAMP mice was assayed using the lactulose/mannitol (Lac/Man) ratio test. Data is expressed as the mean  $\pm$  SEM ( $n = 6-12$  mice per group). (B) 12 week old SAMP-M mice were castrated and then injected i.p. for 6 weeks (daily, 200ul) with vehicle Ctrl (DMSO/PBS), E2 (10  $\mu\text{g}/\text{kg}$ ), PPT (10 mg/kg), or DPN (10 mg/kg). Lac/Man permeability tests were performed following 6-wk treatment and data is expressed as the mean  $\pm$  SEM (\*\* $p < 0.05$ ,  $n = 6$  mice/group).



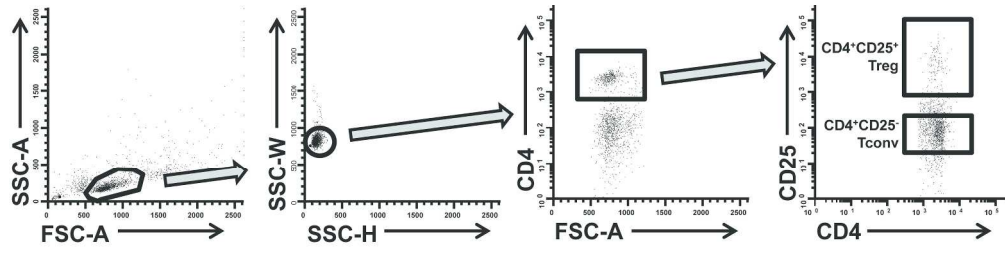
171x123mm (600 x 600 DPI)



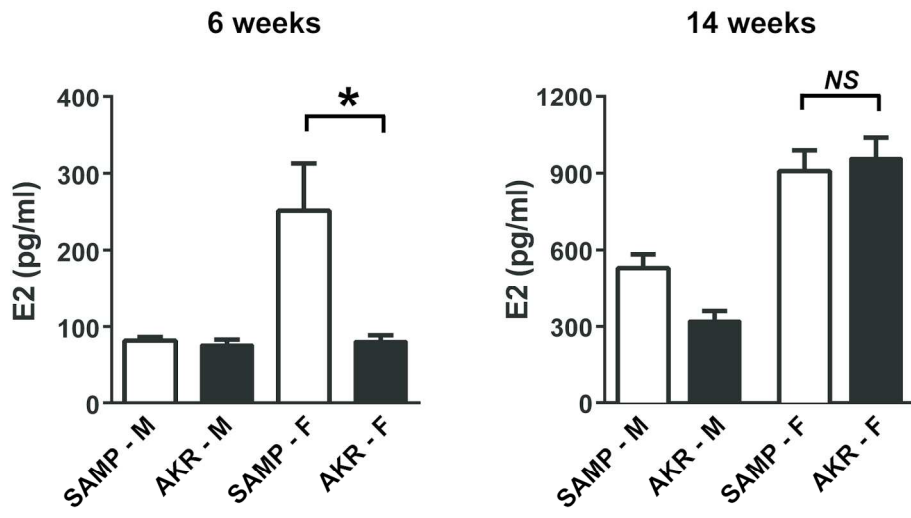
271x66mm (600 x 600 DPI)



199x76mm (600 x 600 DPI)

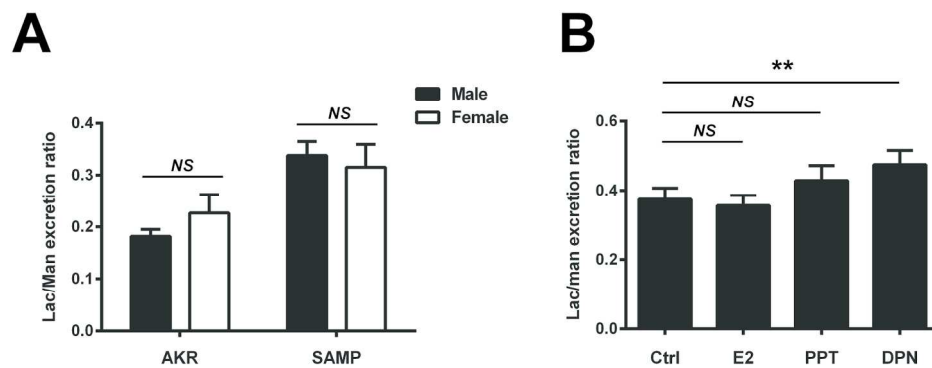


226x55mm (600 x 600 DPI)



165x107mm (600 x 600 DPI)





169x64mm (600 x 600 DPI)